

A robust plasma-based laser amplifier via stimulated Brillouin scattering

E.P. Alves,^{1,*} R.M.G.M. Trines,^{2,*} K.A. Humphrey,³ R. Bingham,^{2,3} R.A. Cairns,⁴ F. Fiúza,⁵ R.A. Fonseca,^{1,6} L.O. Silva,¹ and P.A. Norreys^{7,2}

¹*GoLP/Instituto de Plasmas e Fusão Nuclear, Instituto Superior Técnico, Universidade de Lisboa, 1049-001 Lisbon, Portugal*

²*Central Laser Facility, STFC Rutherford Appleton Laboratory, Didcot, OX11 0QX, United Kingdom*

³*SUPA, Department of Physics, University of Strathclyde, Glasgow, G4 0NG, United Kingdom*

⁴*University of St Andrews, St Andrews, Fife KY16 9AJ, United Kingdom*

⁵*Lawrence Livermore National Laboratory, Livermore, California, USA*

⁶*DCTI/ISCTE Lisbon University Institute, 1649-026 Lisbon, Portugal*

⁷*Department of Physics, University of Oxford, Oxford OX1 3PU, UK*

(Dated: February 6, 2022)

Abstract

It is shown here that Brillouin amplification can be used to produce picosecond pulses of petawatt power. Brillouin amplification is far more resilient to fluctuations in the laser and plasma parameters than Raman amplification, making it an attractive alternative to Raman amplification. Through analytic theory and multi-dimensional computer simulations, a novel, well-defined parameter regime has been found, distinct from that of Raman amplification, where pump-to-probe compression ratios of up to 100 and peak laser fluences over 1 kJ/cm² with 30% efficiency have been achieved. High pulse quality has been maintained through control of parasitic instabilities.

PACS numbers: 52.38.-r, 42.65.Re, 52.38.Bv, 52.38.Hb

Amplification of laser beams via parametric instabilities in plasma (stimulated Raman and Brillouin scattering) has been proposed a number of times [1–5], but came into its own only relatively recently [6–16]. Brillouin scattering has also been used to transfer energy via the Cross-Beam Energy Transfer scheme at the National Ignition Facility [17–23]. Both Raman and Brillouin scattering have been studied extensively in the context of Inertial Confinement Fusion [24–33]; Raman scattering also in the context of wakefield acceleration [34–43]. Raman and Brillouin scattering are processes where two electromagnetic waves at slightly different frequencies propagating in plasma exchange energy via a plasma wave. For Raman scattering, this is a fast electron plasma wave, while for Brillouin scattering it is a slower ion-acoustic wave [44]. When it comes to laser beam amplification, Raman and Brillouin scattering have different properties and serve different purposes. Raman amplification yields the shortest output pulses and the highest amplification ratios, but it is sensitive to fluctuations in the experimental parameters and requires high accuracy in the matching of laser and plasma frequencies. Brillouin amplification yields lower peak intensities or amplification ratios, but is far more robust to parameter fluctuations or frequency mismatch, more efficient (as less laser energy stays behind in the plasma wave) and more suitable for the production of pulses with a high total power or energy.

For both Raman and Brillouin amplification, two main goals can be identified: first, maximising the final power and energy content of the pumped pulse, and second, ensuring that the pumped pulse has the best possible quality, i.e. a smooth envelope and a high contrast (low-intensity pre-pulse). Production of kilojoule, picosecond laser pulses of good quality using Raman amplification has been explored by Trines *et al.* [13, 15]. Here it will be shown that a similar approach also works for Brillouin amplification in the so-called “strong coupling” regime. The lower compression ratios obtained for Brillouin (as compared to Raman) amplification work in favour of this scheme for the production of high-energy picosecond pulses: higher pump intensities can be used to obtain a given probe duration, allowing the use of smaller diameters of the pulses and the plasma column.

To explore how the final duration of a Brillouin-amplified probe pulse can be controlled, we use the self-similar model of Andreev *et al.* [9]. We start from a homogeneous plasma with electron number density n_0 , plasma frequency $\omega_p^2 = e^2 n_0 / (\varepsilon_0 m_e)$, ion plasma frequency $\omega_{pi} = \omega_p \sqrt{Z^2 m_e / m_i}$, electron/ion temperatures T_e and T_i , electron thermal speed $v_T^2 = k_B T_e / m_e$, Debye length $\lambda_D = v_T / \omega_p$, and a pump laser pulse with wave length λ , intensity

I , frequency $\omega_0 = 2\pi c/\lambda$, dimensionless amplitude $a_0 \equiv 8.55 \times 10^{-10} \sqrt{g} \sqrt{I \lambda^2 [\text{Wcm}^{-2} \mu\text{m}^2]}$, where $g = 1$ ($g = 1/2$) denotes linear (circular) polarisation, and wave group speed $v_g/c = \sqrt{1 - \omega_p^2/\omega_0^2} = \sqrt{1 - n_0/n_{cr}}$. Let the durations of pump and probe pulse be given by τ_{pu} and τ_{pr} , and define $\gamma_B = (\sqrt{3}/2)[a_0(v_g/c)\omega_{pi}\sqrt{\omega_0}]^{2/3}$, the Brillouin scattering growth rate in the strong-coupling regime [44]. Then a full expansion of the self-similar coordinate ξ of Ref. [9] yields:

$$a_0(v_g/c)\omega_{pi}\tau_{pr}\sqrt{\omega_0\tau_{pu}} = \sqrt{2g/\eta}\xi_B, \quad (1)$$

where $\xi_B \approx 3.5$ is a numerical constant and η denotes the pump depletion efficiency. The physical interpretation of this expression is that the duration of the probe pulse is similar to the time it takes the probe to deplete the counterpropagating pump: for increasing probe amplification (i.e. longer τ_{pu}) or pump intensity, pump depletion is more rapid and τ_{pr} decreases. This allows one to tune the final probe duration via the properties of the pump beam, similar to Raman amplification [15].

Using the energy balance $a_{pr}^2\tau_{pr} = \eta a_0^2\tau_{pu}$, we also find a relation between amplitude and duration of the growing probe pulse:

$$a_{pr}^2\tau_{pr}^3 = 2g\xi_B^2[\omega_{pi}^2\omega_0(1 - \omega_{pe}^2/\omega_0^2)]^{-1}. \quad (2)$$

We repeat this process for Raman amplification to obtain a similar relation: applying the same energy balance to the Raman self-similar equation $a_0^2\omega_0\omega_p\tau_{pu}\tau_{pr} = (2g/\eta)\xi_M^2$, we find $a_{pr}\tau_{pr} = \sqrt{2g}\xi_M/\sqrt{\omega_0\omega_{pe}}$ with $\xi_M \sim 5$ for a Raman-amplified pulse. This means that the initial probe pulse duration is not a free parameter: Eq. (2) dictates the optimal initial probe pulse duration τ_{opt} for a given initial probe pulse amplitude a_1 . From previous numerical work on Raman [15, 45] and Brillouin amplification [46, 47], it follows that if the probe pulse is too short for its amplitude initially, it will first generate a much longer secondary probe pulse behind the original probe [which does fulfill Eq. (2)] and this secondary probe will then amplify while the original short probe will hardly gain in intensity. Thus, trying to produce ultra-short laser pulses via Brillouin amplification by reducing the initial pulse duration simply does not work. Earlier attempts in this direction [48, 49] showed no increase in total pulse power (as opposed to pulse peak intensity), confirming the results of Ref. [46, 47].

To further investigate Brillouin amplification, in particular limiting factors such as filamentation and wave breaking of the ion wave, we have carried out a sequence of particle-in-cell (PIC) simulations using OSIRIS [50–52]. Parameters varied in these simulations are

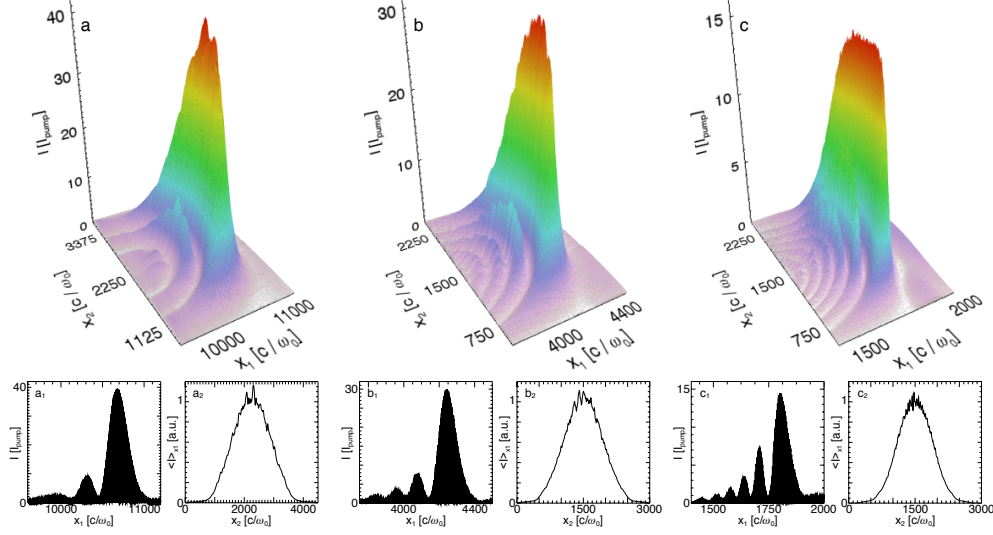


Figure 1: Brillouin-amplified probe pulses for pump/probe intensities of a) 10^{14} , b) 10^{15} and c) 10^{16} W cm^{-2} for $n_0/n_{cr} = 0.3$. Pump pulse durations are 11.4 ps, 3.8 ps and 1.1 ps respectively. The 3D visualizations illustrate the amplified probe pulses at 10% filamentation level. Frames a_1 – c_1 show the longitudinal intensity profile taken at the center of the probe, and frames a_2 – c_2 show the average transverse intensity profile along the longitudinal direction normalized to the average peak intensity.

the pump intensity ($I_0 = 10^{14}$, 10^{15} or 10^{16} W cm^{-2}) and the interaction length. The laser wave length was $\lambda = 1 \mu\text{m}$ and the plasma density was set at $n_0/n_{cr} = 0.3$, to eliminate parasitic Raman scattering. Such scattering can do great damage to the envelope of the amplified pulse, as discussed below. The ion-electron mass ratio was $m_p/m_e = 1836$ and $T_e = T_i = 500$ eV. The initial probe pulse intensity was chosen to be the same as the pump intensity, and the initial probe duration was half the value predicted by (2), because this yielded a somewhat better performance. The plasma column was given a constant density, while the plasma length was determined dynamically as these simulations were conducted in a moving window with the pump pulse implemented as a boundary condition on the leading edge [53].

We have performed two-dimensional moving window simulations, using a spatial resolution of $dx = \lambda_D/2$ and $dy = 0.5c/\omega_0$, with 25 particles per cell per species and quadratic interpolation for the current deposition. Collisions were not included in the simulations: while collisions do induce an intensity threshold on both Brillouin and Raman scatter-

ing, the intensities we use are too far above that for collisions to make much of a difference. Both pump and probe pulses have identical transverse Gaussian envelopes, with waist sizes (W_0) of $W_0 = 1000c/\omega_0 = 160\mu\text{m}$ for the 10^{15} and 10^{16} W cm^{-2} scenarios, and $W_0 = 1500c/\omega_0 = 240\mu\text{m}$ for the 10^{14} W cm^{-2} scenario; these focal spots are chosen to be wide enough to contain > 6 filamentation wavelengths at their respective initial intensity. The probe pulses have \sin^2 temporal profiles, with durations corresponding to $\tau_1 = \tau_{\text{opt}}/2$ determined from (2). The pump pulses have a flat temporal profile with a short rise time of $500 \omega_0^{-1} \simeq 260$ fs.

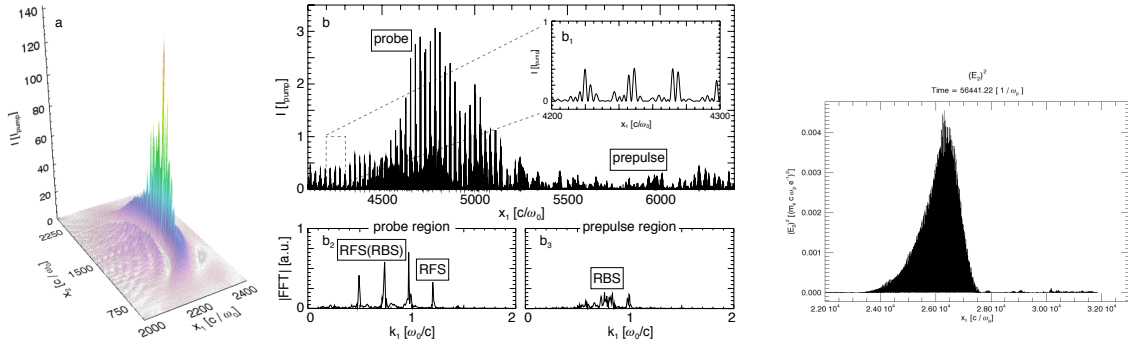


Figure 2: Main parasitic instabilities associated with Brillouin amplification in a) over-quarter-critical ($n_0/n_{cr} = 0.3$) and b) sub-quarter-critical ($n_0/n_{cr} = 0.05$) density regimes. Examples are shown for pump/probe intensities of 10^{16} W cm^{-2} . Distortion of the probe's transverse intensity profile due to filamentation is shown in a). Pump-induced RBS/RFS and probe-induced RFS are shown in b); inset b_1 reveals the development of incoherence at the probe tail, and insets b_2 and b_3 show the spectral signatures of the probe and prepulse regions, respectively. Frame c) shows the amplified probe for $n_0/n_{cr} = 0.01$ and pulse intensities of 10^{15} W cm^{-2} . For this case, the pulse envelope is significantly smoother and the prepulse intensity much lower, even though the interaction time is five times longer than in frame b).

For $n_0/n_{cr} = 0.3$ there will be no Raman backscattering from noise by the pump, i.e. no significant prepulse, and no modulation of the probe pulse envelope by Raman forward scattering. Thus, transverse filamentation of the probe pulse becomes the limiting factor for amplification, while self-focusing and wave breaking are found to be insignificant. The interaction length for each 2-D simulation was chosen such that the probe envelope fluctuations induced by filamentation did not exceed 10% of the probe intensity, leading to pump pulse durations of 11.4 ps, 3.8 ps and 1.1 ps for $I_0 = 10^{14}$, 10^{15} or 10^{16} W cm^{-2}) respectively. Re-

sults are shown in Figure 1. The top row shows the 2-D intensity envelopes of the amplified pulses, while the bottom row shows longitudinal and transverse intensity profiles. The 2-D plots reveal that there is no reduction of the probe pulse diameter, allowing amplification to high total powers, not just high intensities. The intensity envelopes are very smooth, with hardly any fluctuations caused by filamentation or Raman forward scattering. This is in contrast to the results of Refs. [48, 49], which are strongly modulated by filamentation and Raman forward scattering and exhibit a fourfold reduction in spot diameter. Filamentation usually occurs when either the pulse intensities are too high or the interaction length is too long; a typical example of out-of-control filamentation, for a pump pulse at 10^{16} W cm $^{-2}$ and 2 ps duration, is shown in Figure 2(a).

We define the *compression ratio* as the duration of the pump pulse divided by the duration of the amplified probe, and the *amplification ratio* as the intensity of the amplified probe divided by the intensity of the pump. We then find compression ratios of 40, 60 and 72, and amplification ratios of 24, 56 and 70, for pump intensities of 10^{16} , 10^{15} and 10^{14} W cm $^{-2}$ respectively. The increase in these ratios with decreasing pump intensity follows from the fact that the filamentation growth rate scales faster with pulse intensity than the strong-coupling Brillouin scattering growth rate (see below), so using lower pulse intensities allows one to use relatively longer interaction lengths. Of course, using a longer interaction distance may lead to increased premature Brillouin backscattering of the pump before it meets the probe, potentially causing the amplified probe to have a significant prepulse. However, we have shown elsewhere [54] that such premature scattering is strongly damped by collisions, and more so for lower pump intensities that are closer to the collisional threshold for Brillouin scattering. The pump-probe interaction itself is well above this threshold, and therefore much less affected by collisional damping.

We find that the absolute duration of the amplified probe increases with decreasing pulse intensity, as follows from Eq. (1), emphasizing that Brillouin amplification works best for longer pulses at lower intensities. The main peak of the amplified pulse is followed by a sequence of secondary peaks, as predicted by one-dimensional theory and simulations [9, 46, 47]. The amplified pulses have a “bowed” shape, as also seen for Raman amplification [13, 15, 55]. This can easily be explained from the self-similar theory: the pump intensity is highest on-axis and decreases for larger radius, so the probe duration is shortest on-axis and increases for larger radius, leading to the characteristic horseshoe shape. The energy

transfer efficiency is found to be about 30% for each case.

Since filamentation is the most important limiting factor to Brillouin amplification at $n_0/n_{cr} = 0.3$, it has been proposed to reduce filamentation by lowering the plasma density to $n_0/n_{cr} = 0.05$ [48, 49]. However, stimulated Raman scattering is possible at this density, and can be expected to interfere with the amplification process. We carried out a single 1-D static-window simulation at $n_0/n_{cr} = 0.05$ and a plasma column length of 0.8 mm, using pulse intensities of 10^{16} W/cm² and a pump pulse FWHM duration of 2.7 ps, to study the influence of Raman backward and forward scattering on Brillouin amplification; results are displayed in Figure 2(b). Raman backscattering (RBS) was found to generate a large prepulse to the growing probe pulse, spoiling its contrast, while Raman forward scattering (RFS) causes the probe pulse envelope to be strongly modulated, making RFS about as dangerous as filamentation. A Fourier analysis of the k -spectrum of the pulses, shown in Fig. 2(b2) and (b3), reveals that the pump pulse mostly suffers from Raman backward scattering, while Raman forward scattering is dominant in the probe pulse. A close inspection of all Raman scattering occurring during Brillouin amplification found that the growth of the probe pulse saturates due to high levels of Raman forward scattering, rather than Raman backscattering. If the level of RFS in the probe pulse becomes non-linear, the coherence of the probe pulse's carrier wave, and thus the coupling between pump and probe, is lost, and probe amplification stops; this can be seen in Figure 2(b1). Since $\gamma_{RBS} \propto a_0\sqrt{\omega_0\omega_p}$ while $\gamma_{RFS} \propto a_0\omega_p^2/\omega_0$, it follows that growth of RFS and the saturation of the probe pulse are strongly affected by the plasma density, and that lowering this density even further, e.g. to $n_0/n_{cr} = 0.01$, will immediately improve the pump-to-probe amplification ratio and energy transfer, see Figure 2(c). This is mainly due to a reduction in Raman forward scattering: the ramp profile lowers the average density, reducing the RFS growth rate and delaying the saturation of Brillouin scattering. This effect justifies the use of a density ramp to lower the average plasma density and obtain higher amplification gains, as has been observed in Ref. [49]. From this we conclude that Brillouin amplification should be conducted at densities for which RFS is either impossible ($n_0/n_{cr} > 0.25$) or unimportant ($n_0/n_{cr} \leq 0.01$). For $0.01 < n_0/n_{cr} < 0.25$, the disadvantage of increased pump RBS and probe RFS is more serious than the advantage of reduced probe filamentation.

As shown by Andreev *et al.* [9], the Brillouin amplification process is subject to the following scaling laws: $a_{pr}(t) \propto (a_0^2 t)^{3/4}$ and $\tau_{pr}(t) \propto (a_0^2 t)^{-1/2}$, where a_0 is the pump amplitude

and $t = \tau_{pu}/2$ the interaction time. For high plasma densities, where Raman scattering is not possible, the scaling laws can be extended as follows. For the filamentation of the probe pulse, we have $\gamma_f \propto a_{pr}^2$, so $\int \gamma_f dt \propto a_0^3 t^{5/2}$. We can keep the level of filamentation, and thus $\int \gamma_f dt$ constant by choosing $\tau_{pu} \propto I^{-3/5}$, where I denotes the pump intensity. This leads to $\tau_{pr}(t) \propto I^{-1/5}$ and $I_{pr} \propto a_{pr}^2(t) \propto I^{3/5}$. Thus, the compression and amplification ratios both scale as $\tau_{pu}/\tau_{pr} \propto I_{pr}/I \propto I^{-2/5}$ (under the assumption that the efficiency is mostly constant). Finally, we find that the pump pulse energy fluence scales as $F \propto I\tau_{pu} \propto I^{2/5}$. All these scalings are subject to the assumption that one is operating in the strong-coupling regime for Brillouin scattering, $a_0^2 > 4(v_T/c)^3(n_{cr}/n_0)\sqrt{1 - n_0/n_{cr}}\sqrt{Zm_e/m_i}$ or $I_{pu} > 1.6 \times 10^{13} \text{ W cm}^{-2}$ for our parameters. Already it was found that for $I_{pu} = 10^{14} \text{ W cm}^{-2}$, the growing probe did not fully conform to the above scaling laws because I_{pu} is too close to the strong-coupling threshold. Lowering the ion temperature from 500 to 50 eV appears to lower the strong-coupling threshold also, bringing the behaviour of the $I_{pu} = 10^{14} \text{ W cm}^{-2}$ case closer to pure strong-coupling Brillouin amplification and improving its amplification and compression ratios. While ion wave breaking has been observed in one-dimensional simulations [9], with a characteristic time of $\tau_{wb} \propto I^{-1/2}$ [44, 58], it did not play a major role in the two-dimensional simulations presented above, since filamentation always emerged earlier for pump intensities in the strong-coupling regime. From this, it is clear that, when the pump intensity is decreased, Brillouin amplification improves on all fronts.

Previous attempts to study Brillouin amplification in multi-dimensional simulations [48, 49] failed to identify the correct parameter regime for optimal amplification. In Ref. [48], the parameter regime for the initial probe duration τ_1 and the plasma density n_0 is defined as $\tau_{sc} < \tau_1 < \tau_{wb}$ and $n_0/n_{cr} \sim 0.05$, where $\tau_{sc} = 1/\gamma_B$ and τ_{wb} is the wave-breaking time for the ion-acoustic wave [44, 58]. However, a numerical evaluation of τ_{sc} and τ_{wb} in Fig. 1 of Ref. [48] reveals that $\tau_{wb} < \tau_{sc}$, so the two conditions $\tau_{sc} < \tau_1$ and $\tau_1 < \tau_{wb}$ can never be fulfilled simultaneously and the parameter window is empty, while a plasma density of $n_0/n_{cr} = 0.05$ is the worst possible in terms of parasitic Raman scattering (see Fig. 2 above). The ultrashort pulses presented in Refs. [48, 49] do not actually amplify: while their intensity increases by a factor 15, their spot diameter decreases by a factor 4, so their power remains the same. This can be explained by relativistic self-focusing, enhanced by the presence of the pump pulse [59, 60]. Also, it is shown in Fig. 3b of Ref. [49] that

switching off ion motion makes no significant difference to the intensity gain of these ultra-short pulses, thus ruling out Brillouin amplification (which requires the presence of an ion wave) as a contributing factor to the pulse evolution. For the various longer-pulse cases discussed in Refs. [48, 49], we find that n_0 , I_{pu} and $a_1^2 \tau_{pr}^3$ are all kept constant, so these cases represent various stages of a single configuration, rather than independent configurations, and therefore do not constitute a true parameter scan.

In conclusion, we have studied strong-coupling Brillouin amplification of short (~ 0.1 ps) laser pulses in plasma. Amplification factors of up to 40 have been obtained for moderate pump intensities (10^{14} W cm $^{-2}$) and high plasma densities ($n_0/n_{cr} = 0.3$). Notable achievements of this paper constitute: (i) the self-similar equations (1) and (2), which govern the evolution of the growing probe versus the pump pulse intensity, the plasma density and the interaction length; (ii) the identification of the plasma density and the pump pulse intensity as the free parameters of the problem, while the initial probe pulse duration is a dependent parameter; (iii) the use of multi-dimensional simulations to Brillouin-amplify pulses to high power, while preserving pulse quality and contrast, where previous work mostly focused on high intensity and ignored pulse quality; (iv) the identification of filamentation and probe RFS as the critical limiting instabilities; (v) a study of parasitic Raman back- and forward scattering in Brillouin amplification for $n_e/n_{cr} < 0.25$, highlighting their deleterious influence on the quality and contrast of the amplified probe pulse; (vi) identification of the following parameter regime for efficient, high-quality Brillouin amplification: $I_{\text{pump}} < 10^{15}$ W cm $^{-2}$ and $n_e/n_{cr} > 0.25$, with $n_e/n_{cr} \leq 0.01$ as an alternative; (vii) scaling laws for the various probe pulse parameters after amplification, showing that Brillouin amplification improves on all fronts when the pump pulse intensity is lowered. Together, these results show that, for the right laser-plasma configurations, Brillouin amplification is a robust and reliable way to compress and amplify picosecond laser pulses in plasma, and provide a comprehensive guide for the design and execution of future Brillouin amplification experiments.

This work was supported financially by STFC and EPSRC, by the European Research Council (ERC-2010-AdG Grant 167841) and by FCT (Portugal) grant No. SFRH/BD/75558/2010. We would like to thank R. Kirkwood and S. Wilks for stimulating discussions. We acknowledge PRACE for providing access to SuperMUC based in Germany at the Leibniz research center. Simulations were performed on the Scarf-Lexicon Cluster (STFC RAL) and SuperMUC (Leibniz Supercomputing Centre, Garching, Germany).

* Authors E. Alves and R. Trines contributed equally to this work.

- [1] M. Maier, W. Kaiser, and J. A. Giordmaine, Phys. Rev. Lett. **17**, 1275 (1966).
- [2] R. D. Milroy, C. E. Capjack, and C. R. James, Plasma Phys. **19**, 989, (1977).
- [3] R. D. Milroy, C. E. Capjack, and C. R. James, Phys. Fluids **22**, 1922 (1979).
- [4] C. E. Capjack, C. R. James, and J. N. McMullin, J. Appl. Phys. **53**, 4046 (1982).
- [5] A. A. Andreev and A. N. Sutyagin, Sov. J. Quantum Electron. **19**, 1579 (1989).
- [6] V.M. Malkin, G. Shvets and N.J. Fisch, Phys. Rev. Lett. **82**, 4448 (1999).
- [7] R. Kirkwood *et al.*, Phys. Rev. Lett. **83**, 2965 (1999).
- [8] Y. Ping *et al.*, Phys. Rev. Lett. **92**, 175007 (2004).
- [9] A.A. Andreev *et al.*, Phys. Plasmas **13**, 053110 (2006).
- [10] J. Ren *et al.*, Nature Physics **3**, 732-736 (2007).
- [11] Y. Ping *et al.*, Phys. Plasmas **16**, 123113 (2009).
- [12] L. Lancia *et al.*, Phys. Rev. Lett. **104**, 025001 (2010).
- [13] R.M.G.M. Trines *et al.*, Nature Physics **7**, 87 (2011).
- [14] R.K. Kirkwood *et al.*, Phys. Plasmas **18**, 056311 (2011).
- [15] R.M.G.M. Trines *et al.*, Phys. Rev. Lett. **107**, 105002 (2011).
- [16] Z. Toroker, V. M. Malkin and N. J. Fisch, Phys. Rev. Lett. **109**, 085003 (2012).
- [17] W.L. Kruer *et al.*, Phys. Plasmas **3**, 382 (1996).
- [18] E.A. Williams *et al.*, Phys. Plasmas **11**, 231 (2004).
- [19] P. Michel *et al.*, Phys. Plasmas **16** 042702 (2009).
- [20] S.H. Glenzer *et al.*, Science **327**, 1228 (2010).
- [21] P. Michel *et al.*, Phys. Plasmas **17** 056305 (2010).
- [22] D.E. Hinkel *et al.*, Phys. Plasmas **18** 056312 (2011).
- [23] J.D. Moody *et al.*, Nature Physics **8**, 344 (2012).
- [24] K. Tanaka *et al.*, Phys. Rev. Lett. **48**, 1179 (1982).
- [25] C.J. Walsh, D.M. Villeneuve and H.A. Baldis, Phys. Rev. Lett. **53**, 1445 (1984).
- [26] D. M. Villeneuve, H. A. Baldis, and J. E. Bernard, Phys. Rev. Lett. **59**, 1585 (1987).
- [27] W.B. Mori *et al.*, Phys. Rev. Lett. **72**, 1482 (1994).
- [28] A. B. Langdon and D. E. Hinkel, Phys. Rev. Lett. **89**, 015003 (2002).

- [29] J.D. Lindl *et al.*, Phys. Plasmas **11** 339 (2004).
- [30] D.E. Hinkel *et al.*, Phys. Plasmas **12**, 056305 (2005).
- [31] D.H. Froula *et al.*, Phys. Plasmas **14**, 055705 (2007).
- [32] P. Michel *et al.*, Phys. Rev. E **83**, 046409 (2011).
- [33] S.H. Glenzer *et al.*, Phys. Rev. Lett. **106**, 085004 (2011).
- [34] D.W. Forslund *et al.*, Phys. Rev. Lett. **54**, 558 (1985).
- [35] C.D. Decker, W.B. Mori and T. Katsouleas, Phys. Rev. E **50**, R3338 (1994).
- [36] C. Rousseaux *et al.*, Phys. Rev. Lett. **74**, 4655 (1995).
- [37] K. Krushelnick *et al.*, Phys. Rev. Lett. **75**, 3681 (1995).
- [38] K.-C. Tzeng, W.B. Mori, and C.D. Decker, Phys. Rev. Lett. **76**, 3332 (1996).
- [39] C.D. Decker *et al.*, Phys. Plasmas **3**, 1360 (1996).
- [40] C.I. Moore *et al.*, Phys. Rev. Lett. **79**, 3909 (1997).
- [41] K.-C. Tzeng and W.B. Mori, Phys. Rev. Lett. **81**, 104 (1998).
- [42] D. Gordon *et al.*, Phys. Rev. Lett. **80**, 2133 (1998).
- [43] T. Matsuoka *et al.*, Phys. Rev. Lett. **105**, 034801 (2010).
- [44] D.W. Forslund, J.M. Kindel and E.L. Lindman, Phys. Fluids **18**, 1002-1016 (1975).
- [45] J. Kim, H.J. Lee, H. Suk and I.S. Ko, Phys. Lett. A **314**, 464 (2003).
- [46] G. Lehmann, K. H. Spatschek and G. Sewell, Phys. Rev. E **87**, 063107 (2013).
- [47] G. Lehmann and K. H. Spatschek **20**, 073112 (2013).
- [48] S. Weber *et al.*, Phys. Rev. Lett. **111**, 055004 (2013).
- [49] C. Riconda *et al.*, Phys. Plasmas **20**, 083115 (2013).
- [50] R.A. Fonseca, L.O. Silva, F.S. Tsung, *et al.*, Lect. Not. Comp. Sci. **2331**, 342-351 (2002).
- [51] R. A. Fonseca, L. O. Silva, J. Tonge *et al.*, Phys. Plasmas **10**, 1979 (2003).
- [52] R. A. Fonseca, S. F. Martins, L. O. Silva *et al.*, Plasma Phys. Contr. Fusion, **50**, 12 (2008).
- [53] P. Mardahl *et al.*, Bull. Am. Phys. Soc. **46**, DPP 2001, KP1.108 (2001); P. Mardahl, Ph.D. thesis, University of California, Berkeley (2001).
- [54] K.A. Humphrey, R.M.G.M. Trines *et al.*, Phys. Plasmas **20**, 102114 (2013).
- [55] G. M. Fraiman, N. A. Yampolsky, V. M. Malkin and N. J. Fisch, Phys. Plasmas **9**, 3617 (2002).
- [56] P. Kaw, G. Schmidt, and T. Wilcox, Phys. Fluids **16**, 1522 (1973).
- [57] C.E. Max, J. Arons and A.B. Langdon, Phys. Rev. Lett. **33**, 209 (1974).

- [58] S. Hüller, P. Mulser and A. M. Rubenchik, Phys. Fluids B **3**, 3339 (1991).
- [59] C. Joshi, C.E. Clayton and F.F. Chen, Phys. Rev. Lett. **48**, 874 (1982).
- [60] G. Shvets and A. Pukhov, Phys. Rev. E **59**, 1033 (1999).